Appendix 6
Common MRS Artifacts

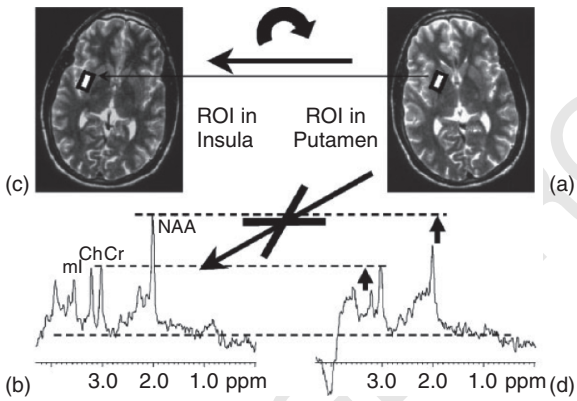

Figure 1. The body shifts relative to voxel location in single voxel MRS.[1] A single point resolved spectroscopy (PRESS) voxel was placed in the putamen based on a localizer image (a), and an ^{1}H spectrum (b) was acquired. However, unknown to the operator, the subject had turned his head to the left, as evidenced on a localizer scan repeated after the MRS acquisition (c). Owing to the movement, the voxel targeted at the putamen resulted in a spectrum being acquired from insular gray matter (GM) instead, with narrow lines atypical of basal ganglia. A spectrum subsequently acquired from the putamen (d) shows that a completely wrong diagnosis would have resulted if the spectrum from insular GM was assumed to originate from putamen. Thus, verification of proper voxel placement is crucial. (Scan parameters: 26-year-old man; magnetic resonance imaging, MRI: fast spin echo sequence, echo train length 16, repetition time TR = 3 s, echo time TE = 100 ms; MRS: voxel size = 2.2 cm^3, TE = 20 ms, TR = 3 s, number of acquisitions, NEX = 128; NAA = *N*-acetylaspartate, Cr = total creatine; Ch = total choline, and mI = myo-inositol). (Reproduced with permission from Ref. 1. © John Wiley & Sons, Ltd., 2004.)

Handbook of Magnetic Resonance Spectroscopy In Vivo: MRS Theory, Practice and Applications.
Edited by Paul A. Bottomley and John R. Griffiths,
© 2016 John Wiley & Sons, Ltd. ISBN: 978-1-118-99766-6

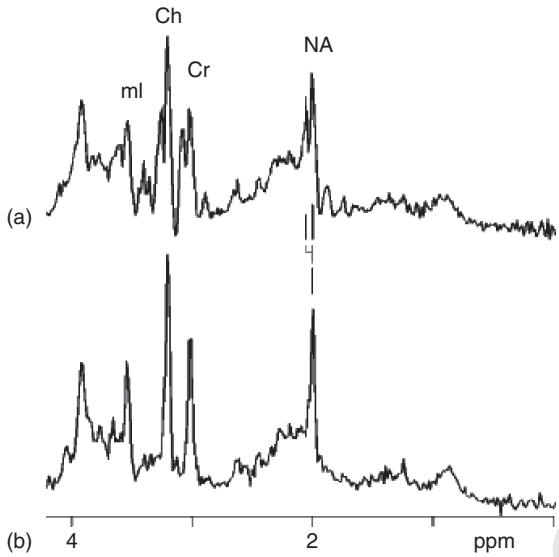

Figure 2. Effect of movement between two locations in single voxel MRS.[1] (a) All of the peaks are split in this ^{1}H PRESS spectrum from a neonate (gestational age, 41 weeks) who moved his/her head between two distinct positions during the scan.[2] (b) A repeat examination, acquired with the baby soundly asleep, eliminates the motion-induced splittings and lineshape distortion (voxel in the thalamus, TE = 20 ms, TR = 2 s, NEX = 128, and NA = NAA). (Reproduced with permission from Ref. 1. © John Wiley & Sons, Ltd., 2004.)

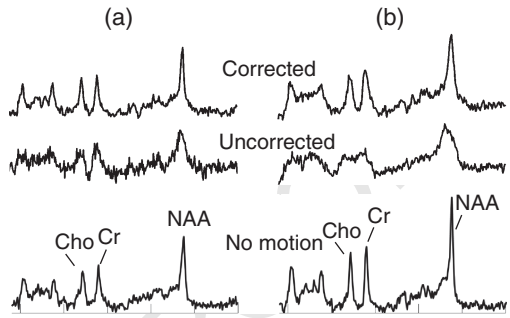

Figure 3. Effect of random motion on single voxel MRS.[3] Single voxel ^{1}H spectra were acquired from a 4-ml voxel in frontal white matter (WM) from two subjects (a) and (b), collecting and saving NEX = 128 echo signals separately. The bottom spectra were obtained from a conventional average of the 128 echo signals with the subjects lying still. The center traces were obtained the same way but during moderate (~1.5 cm; left) and severe (>4 cm; right) random right-left head rotations. The lines are broadened and the signal-to-noise ratio (SNR) degraded significantly by phase cancellation and frequency shifts caused by the motion. In the top spectra, each individual echo signal is phase-corrected and aligned in frequency before averaging. In this example the alignment in phase and frequency was easily accomplished because the spectra were acquired with the metabolite cycling technique, i.e. without water presaturation[4,5]. This procedure substantially improved the SNR and linewidths. This 'constructive averaging' can also be based on the metabolite signals[6], as demonstrated for GABA editing.[7]

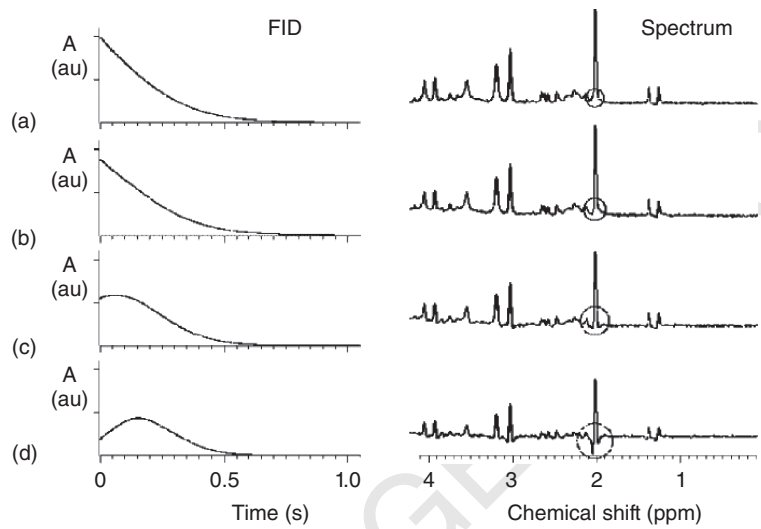

Figure 4. Effect of unbalanced gradient pulses on lineshape in single voxel MRS.[1] Unbalanced gradient crusher pulses in combination with B_0 gradients shift the echo maximum away from the echo time at which spin–spin (T_2) refocusing occurs in a PRESS ^{1}H voxel (TE = 20 ms, TR =3 s; FID = free induction decay) from a phantom solution of phosphate-buffered metabolites (NAA, Cr, Ch, mI, glutamate, lactate, sodium azide, and gadolinium-diethylenetriaminepentaacetate; obtained from GE Medical Systems, Milwaukee, USA). The shifted echoes result in 'negative feet' for each peak (circled). The shift of the double spin echo was provoked by misadjusting the relative amplitudes of PRESS crusher gradients followed by manual shimming to maximize peak intensities. (a) FID and spectrum from a correctly adjusted sequence. In parts (b)–(d), gradient amplitudes are increasingly unbalanced, leading to net peak areas of 89%, 56%, and 19% compared to (a), respectively. (Reproduced with permission from Ref. 1. © John Wiley & Sons, Ltd., 2004.)

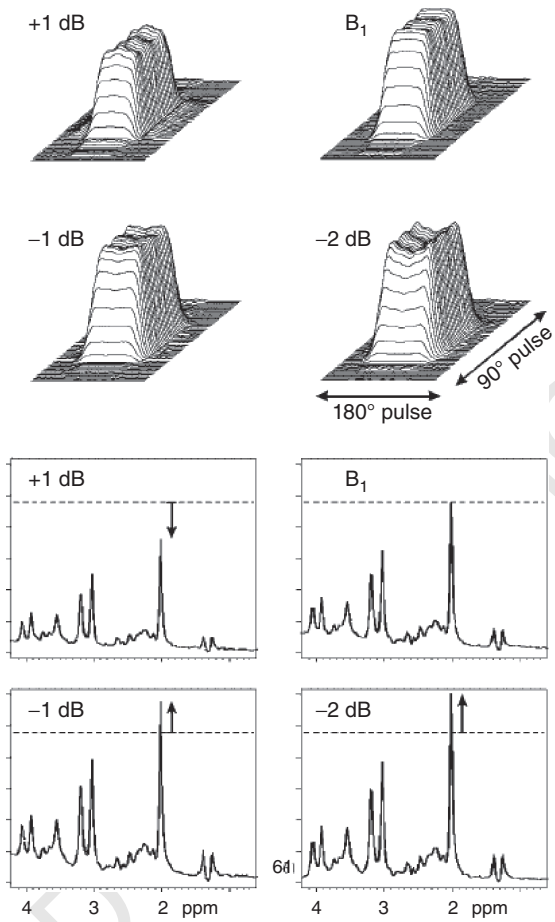

Figure 5. Effect of radio-frequency (RF) pulse amplitude on voxel profile.[1] The effect of transmit power levels on real-world voxel profiles from a calibration phantom applying a commercial PRESS sequence optimized for short echo time are shown at top. The automatic prescan procedure on a GE Medical Systems (Milwaukee, USA) 1.5 T scanner adjusted the RF voltage to produce the single voxel ROI profile labeled B_1. Deliberate misadjustment of the RF transmit voltage by ± 1 dB and -2 dB yielded the other three profiles that exhibit less uniform excitation within the voxel and increased excitation of regions outside the voxel. The corresponding ^{1}H spectra, below, show that the best excitation profile does not yield the maximum signal. (Scan parameters: TE = 35 ms, TR = 2 s, numerically optimized excitation pulses implemented; no outer volume saturation (OVS), or reduced flip-angle pulses). (Reproduced with permission from Ref. 1. © John Wiley & Sons, Ltd., 2004.)

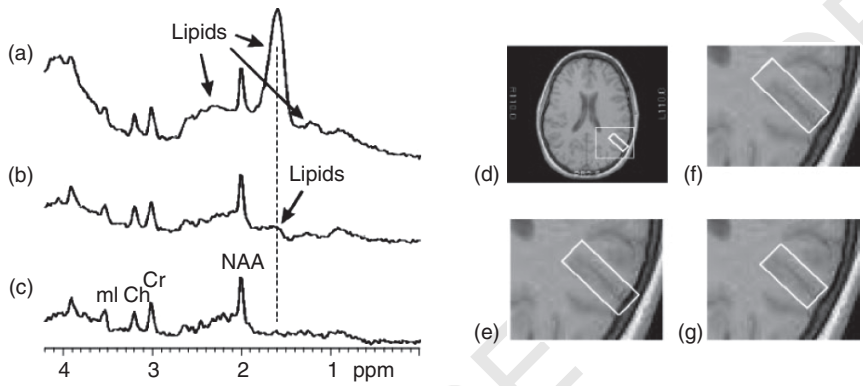

Figure 6. Lipid contamination from imperfect slice selection in single voxel MRS.[1] Signal from outside a selected single voxel can give dominating ^{1}H signal contributions if the transition zones of the slice-selective pulses fall in regions with intense lipid signals. These PRESS spectra (a–c) were obtained from a 40-year-old woman. The voxel was 10 mm × 15 mm × 27 mm in (a) and (b) and the spectra show significant lipid contamination, corresponding to images (e) and (f), respectively. Moving the voxel away from the skull in (f), did not completely eliminate the lipid contamination in spectrum (b). However, reducing the voxel size to 10 mm × 15 mm × 22 mm for spectrum (c) diminished the transition zone in the longest dimension toward the lipid-bearing scalp, causing the lipid contribution to vanish. (Scan parameters: TE = 20 ms, TR = 3 s, 1953 Hz spectral width, 1024 points zero-filled to 2048 points, no OVS). (Reproduced with permission from Ref. 1. © John Wiley & Sons, Ltd., 2004.)

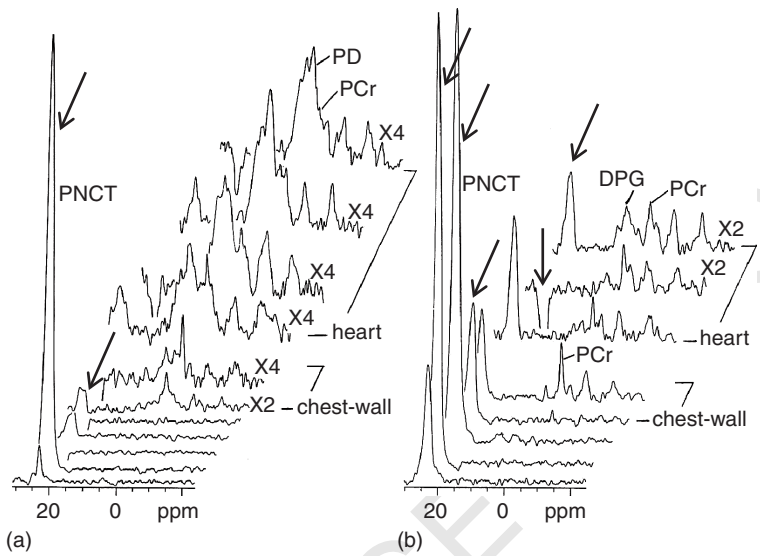

Figure 7. Signal bleed from imperfect point spread function (PSF) in one-dimensional (1-D) chemical shift imaging (CSI).[8] These 1-D ^{31}P CSI data sets were acquired sequentially with a surface coil on the chest of a heart transplant patient (a) and a normal volunteer (b) at 1.5 T in about 10 min with uniform excitation.[8] They are plotted as a function of depth through the chest with a spatial resolution of 1 cm. A 1-cm vial containing a saturated solution of phosphonitrilic chloride trimer (PNCT) was embedded in the surface coil as a marker. In (a), the vial is centered almost perfectly in a CSI voxel, so the PSF samples the PNCT signal near the center of the voxel. Therefore, adjacent voxels lie close to the zero-crossing points of the PSF and produce minimal 'bleed' artifacts in adjacent voxels (arrows). In (b) however, the vial is displaced several millimeter relative to the scanner (by the subject's weight), so that the center-of-mass of the PNCT signal falls between two adjacent voxels in the laboratory frame-of-reference. The PSF side lobes are now sampled near their maxima, resulting in intense PNCT signal bleeding into all of the CSI voxels. The phase of the bleed signal alternates as it traces out the sinc-function-shaped PSF profile (arrows). The bleed can be minimized by offsetting the phase in the spatial Fourier transform (FT), which is equivalent to shifting the CSI grid, so that the PNCT vial falls at the center of the voxel (PD = phosphodiesters, DPG =blood 2,3-diphosphoglycerate, and PCr = phosphocreatine). (Reproduced with permission from Ref. 5. © John Wiley & Sons, Ltd., 1989.)

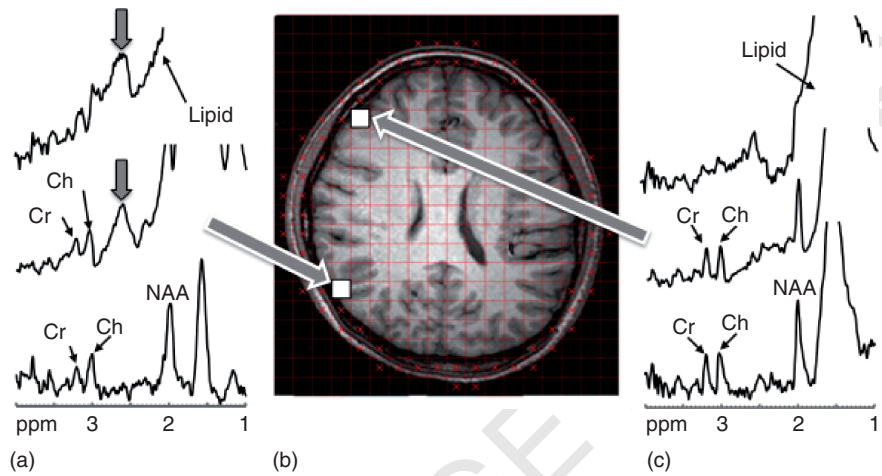

Figure 8. Lipid signal bleed from imperfect point spread function (PSF) in two-dimensional (2-D) CSI. The same effect as in Figure 7 is illustrated here in two voxels from the periphery of the brain (b; white squares) extracted from a 2-D ^{1}H CSI data set acquired from a normal volunteer at 3 T with $1 \times 1 \times 1.5$ cm resolution.[9] In the conventional CSI reconstruction, both spectra (a, c; top) are swamped by intense lipid signal from adjoining voxels in the scalp that obliterate the NAA, Ch and Cr peaks and introduce artifact peaks (arrows). Application of a spatial cosine filter reduces the lipid artifact (center spectra) so that the Cr and Ch peaks are at least observable—as well as NAA in (c), albeit at the expense of spatial resolution. The lipid peak remains problematic for quantification. Independently moving the spatial locations of lipid-bearing voxels (b; voxels with crosses) by iteratively offsetting the phase in the spatial 2-D FT CSI reconstruction reduces the lipid contamination enabling clean resolution of NAA in the peripheral brain without degrading resolution (bottom spectra).[9] This optimization moves the lipid signal centers-of-mass close to the voxel centers so that the PSF is sampled close to zero-crossings in adjacent voxels.

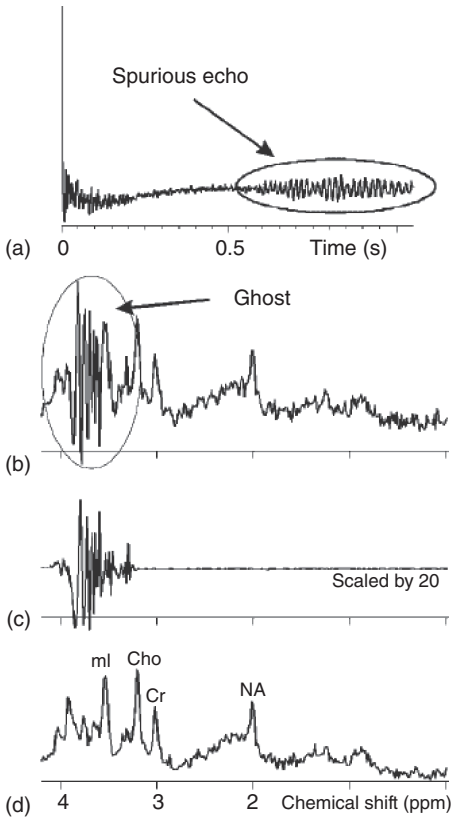

Figure 9. Effect of spurious echoes.[1] If the gradient crusher pulse amplitudes are too weak and local B_0 inhomogeneities are significant, unwanted echo signals can be generated by multiecho sequences such as PRESS. (a) An ^{1}H FID from a PRESS acquisition (TE = 20 ms, TR = 3 s) from developing WM in a female preterm neonate (34 weeks gestational age) with an unwanted echo (circled). (b) The typical appearance of spurious echoes or 'ghosts', in the spectrum. Because extended phase cycling was used for data acquisition, the origin of the spurious signal could be identified as arising from the two-pulse echo from the initial 90° and last 180° pulse, by FT along the phase-rotation dimension (c). In this case, the ghosting artifact was eliminated by zeroing the latter half of the FID as shown in (d). The same ghost signals in (b) can be identified from the residuals obtained after fitting the spectrum with the LC-model (see Chapter 18),[2] permitting differentiation of the individual metabolite signals. (Reproduced with permission from Ref. 1. © John Wiley & Sons, Ltd., 2004.)

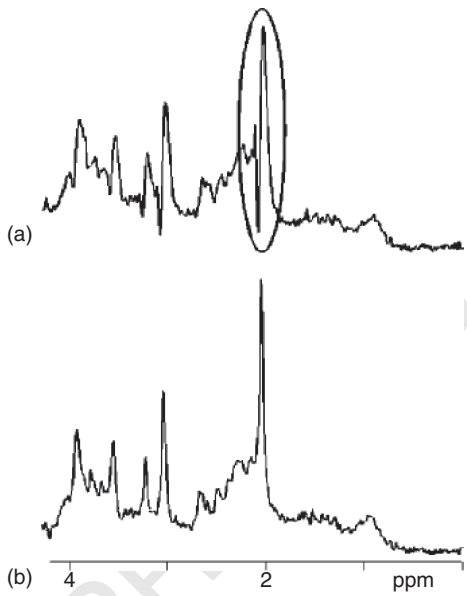

Figure 10. Effect of eddy currents.[1] All lineshapes are distorted in (a) due to eddy currents from the localizing gradients in this short-TE PRESS ^{1}H spectrum (TE = 20 ms) from occipital GM in a 14-year-old boy. (b) The same spectrum after restoration of the lineshape using the phase information. (Reproduced with permission from Ref. 1. © John Wiley & Sons, Ltd., 2004.)

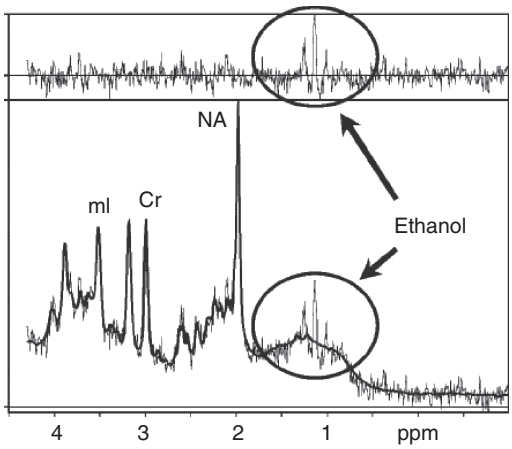

Figure 11. Unexpected resonances in the fitting residuals[1]. An ^{1}H spectrum of parietal WM from a 41-year-old male subject was fitted with LC-model using a standard basis set. The original spectrum and its fit are plotted in the lower panel. The residuals after subtracting the fitted spectrum in the upper panel show signals not attributable to noise that can identify unexpected metabolites in patients (in this case, the triplet is due to ethanol consumed before the scan).[10] (Reproduced with permission from Ref. 1. © John Wiley & Sons, Ltd., 2004.)

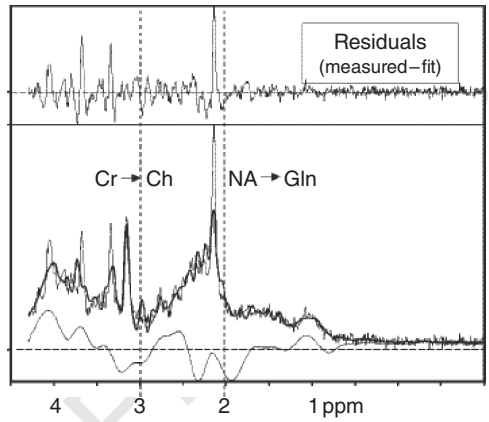

Figure 12. Incorrect peak assignments.[1] The importance of knowing and controlling peak assignment is illustrated by this case of an ^{1}H spectrum frequency-shifted and compared with its usual position. The fitting algorithm was unable to correct for the frequency shift and converged to an incorrect minimum wherein the spectral peaks were wrongly assigned. This yielded absurd quantitative metabolite levels: the Cr peak was interpreted as Ch, and NAA was quantified mainly as glutamine (Gln) with [Cr] = 0.4 mM instead of 6.2 mM and for [Gln] = 20 mM instead of 1 mM. Checking fitting residuals and the baseline for plausibility, avoids such misassignments in near-normal spectra. However, in abnormal spectra (e.g., tumors, where NAA may be missing, and Cr may be low), correct assignments are more difficult to verify (Gln = glutamine). (Reproduced with permission from Ref. 1. © John Wiley & Sons, Ltd., 2004.)

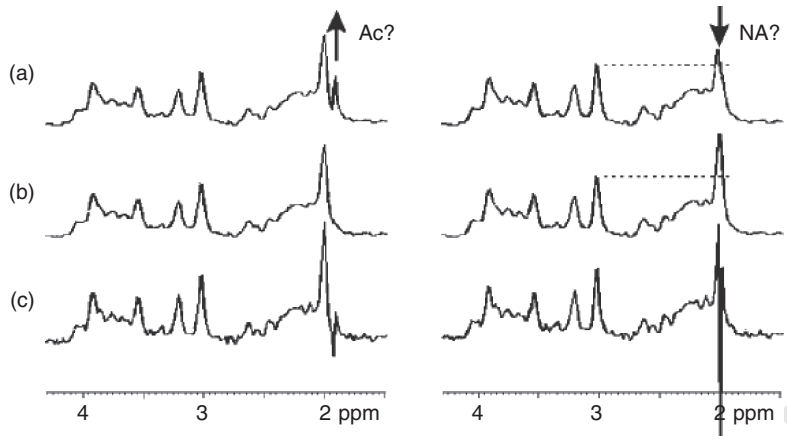

Figure 13. Spurious RF signals.[1] The effect of an RF leak that adds a constant external RF signal to the FID is demonstrated in a PRESS (perisylvian GM) ^{1}H spectrum from a 9-year-old boy with 2 Hz apodization. In the left-hand spectra in (a) and (c), an external low-level RF signal was applied at 1.93 ppm where it could easily be mistaken for acetate. This is evident in the minimally treated spectrum (c; left) where the added signal is sharper and out of phase with the rest of the spectrum but not in the smoothed spectrum (a; left). In the right-hand spectra, the external RF signal overlaps NAA at about 2.0 ppm. Again, the minimally treated spectrum (c; right) shows a sharp artifact because the external signal does not decay with T_2. However, if only the line-broadened spectrum (a; right) is inspected, the artifact is easily missed, and the spectrum could suggest neurodegeneration. (Reproduced with permission from Ref. 1. © John Wiley & Sons, Ltd., 2004.)

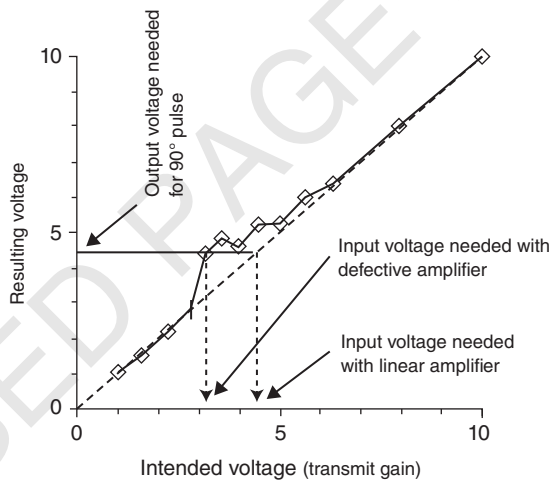

Figure 14. Effect of nonlinear power amplification.[1] The transmit gain, expressed as a voltage and adjusted by auto-prescan or the operator, normally translates linearly to the output voltage and current for generating the transverse field, B_1, after power amplification (dashed diagonal line). Hence, the transmit gain can be used to calculate B_1 needed for quantification based on the reciprocity principle (see Chapter 1). However, in this case, power amplification was defective (diamond symbols), producing a nonlinear jump in output with a small increase in transmit gain over a portion of its range. If the reciprocity principle were used for determining coil sensitivity for quantification, metabolite concentrations could be underestimated by up to 30%. (Reproduced with permission from Ref. 1. © John Wiley & Sons, Ltd., 2004.)

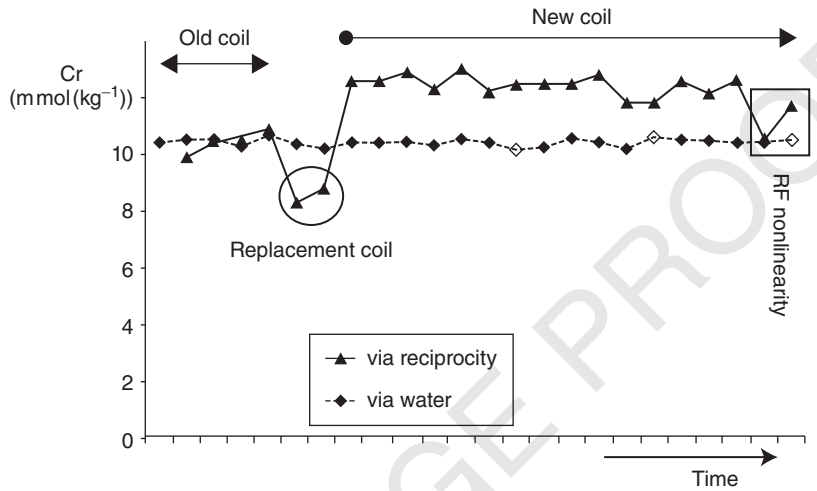

Figure 15. Detection of hardware failure from regular phantom MRS studies.[1] The plot shows the total creatine content of a phantom (cf. Figure 4) determined by two methods as a function of time. Method 1 (diamonds) used the water signal as an internal concentration reference. As expected for a stable solution, these values do not fluctuate. However, values measured through application of the reciprocity principle (triangles) exhibit larger fluctuations that can be symptomatic of hardware failure or deterioration, in particular in this example RF coil failure and amplifier nonlinearity. If reciprocity is being used to obtain quantitative values from clinical examinations, phantom measurements are indispensable for recalibration after changes in hardware and detecting its incipient failure, as well as ensuring that system SNR has not deteriorated. (Reproduced with permission from Ref. 1.)

John R. Griffiths
University of Cambridge, Cambridge, UK

Roland Kreis
University of Bern, Switzerland

Paul A. Bottomley
Johns Hopkins University, Baltimore, MD, USA

REFERENCES

1. R. Kreis, *NMR Biomed.*, 2004, **17**, 361.
2. http://www.s-provencher.com/pages/lcmodel.shtml.
3. E. L. MacMillan, M. Bortolotti, A. Boss, C. Boesch, and R. Kreis. *Proc. Intl. Soc. Mag. Reson. Med.*, 2011, **19**, 2996.
4. R. A. De Graaf, In vivo NMR spectroscopy Principles and Techniques, 2nd edition, John Wiley & Sons, Chichester UK, 2007, p 450.
5. E. L. MacMillan, D. G. Chong, W. Dreher, A. Henning, C. Boesch, and R. Kreis. *Magn. Reson. Med.*, 2011, **65**, 1239.
6. R. E. Gabr, S. Sathyanarayana, M. Schär, R. G. Weiss, and P. A. Bottomley, *Magn. Reson. Med.*, 2006, **56**, 754.
7. R. Simpson, G. A. Devenyi, P. Jezzard, and T. J. Hennessy. *J. Near, Magn. Reson. Med.*, 2015, doi: 10.1002/mrm.26091.
8. P. A. Bottomley, C. J. Hardy, P. B. Roemer, and R. G. Weiss, *NMR Biomed.*, 1989, **2**, 284.
9. Y. Zhang, J. Zhou, and P. A. Bottomley, *Magn. Reson. Med.*, 2014, **74**, 320.
10. R. Kreis, L. Hofmann, and C. Boesch, *Proc. Intl. Soc. Mag. Reson Med.*, 2000, **8**, 426.